Relationships Between Microstructure, Fracture–Surface Morphology, and Mechanical Properties in Ethylene and Propylene Polymers and Copolymers

FABRICE LAPIQUE, PAUL MEAKIN, JENS FEDER, TORSTEIN JØSSANG

Department of Physics, University of Oslo, Box 1048, Oslo 0316, Norway

Received 26 May 1999; accepted 10 September 1999

ABSTRACT: The fracturing of four different polyolefin materials (a polypropylene homopolymer, a propylene–ethylene copolymer, a polyethylene homopolymer, and an ethylene–hexene copolymer) was studied with the objective of developing a better understanding of the relationships between the morphology of semicrystalline polymers, the morphology and growth kinetics of their fracture surfaces, and their mechanical properties. A scanning electron microscope and an optical microscope were used to obtain images of the fracture surfaces. The samples were injection-molded or hot-pressed to generate different microstructures. Fracture experiments were performed at 23, 0, and −20°C to generate fracture surfaces with different morphologies from the same supermolecular structure. It appears that the fracture propagates through the spherulites in a brittle manner. The macroscopic aspect of the fracture surfaces is temperature-independent and changes are visible only at the microscopic scale. Over the range of temperatures studied, the rms roughness [root mean square roughness $= \sqrt{1/n \sum_{i=n}^{n} (Z_i - \bar{Z})^2}$] decreased by only about 20%, while the fracture energy of all but one of the materials (a high-density ethylene–hexene copolymer) decreased by about 60% as the temperature was reduced. © 2000 John Wiley & Sons, Inc. J Appl Polym Sci 77: 2370–2382, 2000

Key words: fracture; microstructure; polypropylene; polyethylene; fracture energy

INTRODUCTION

The main objective of the work described in this paper was to study the relationships between the morphology of commercially important polymers, the morphology and growth kinetics of their fracture surfaces, and their mechanical properties. Exploration of the relationships between the supermolecular structure, the fracture surface topography, and the fracture performance presents very exciting challenges, from both a basic research and an industrial point of view. We studied the relationships between the morphology of materials and the mechanical properties of products manufactured from them through the characterization of the fracture surface. The polymer morphology/microstructure can be described in terms of crystallinity, crystal-size distribution, density, molecular weight distribution, and chain-branch density. If a link between the molecular structure and mechanical properties can be established, new concepts could be developed to design polymers with superior properties. The materials that were studied are polyolefins (polyethylene and polypropylene), commercially very important polymers. International standardized procedures (ISO standard) for industrial test procedures were followed in the fracture experi-

Correspondence to: F. Lapique, SINTEF, P.B. 124 Blindern, N-0314 Oslo, Norway (Fabrice.Lapique@matek.sintef.no).

Journal of Applied Polymer Science, Vol. 77, 2370–2382 (2000)

ments. Scanning electron microscopy (SEM) and optical microscopy were used to qualitatively characterize the fracture surfaces.

BACKGROUND

When a crack propagates, stress is concentrated at its tip. The stress near the tip becomes higher than the yield stress, and a plastic zone develops in front of the advancing tip. Under certain conditions, cavitation and fibrillation processes occur in this zone. This phenomenon is known as crazing. Crazes, unlike cracks, are load bearing because their two surfaces are bridged by small fibrils with diameters in the range 5 to 30 μm. When a fracture propagates, it does so by breakdown of the fibril structure within the craze, a process that is supported by the high local stress in the fibrils. Crazing can be very beneficial, because it is an energy-absorbing plastic-deformation process. This and other plastic-deformation processes are the most important sources of fracture toughness, G_c.

A complex sequence of events can be expected to take place during craze formation in bulk semicrystalline polymers.[1] At sites of enhanced stress concentration, local sliding occurs between individual lamellar ribbons. This process is facilitated by the low degree of entanglements in the common amorphous interlayer between the lamellar ribbons. During this stage, strain is accommodated almost entirely by the interlamellar amorphous regions. At the same time, the crystals change their orientation and the shear component decreases, while the stress in the direction of the molecular axis of the crystals increases. Once the local stress reaches a critical value (equal to the stress at which macroscopic yielding can take place), individual blocks are pulled out of the crystal ribbons. Due to this local yielding process, submicroscopic defects are created between the lamellae. In the as-formed condition, the fibrils consist of partly extended tie-molecules with occasional blocks of still folded crystal between the strings.

In view of the complex processes that take place during deformation, it is apparent that processing conditions, especially heat treatment and cooling rate, can influence the mechanical properties of products manufactured from semicrystalline polymers. Processing conditions determine the crystallinity and crystal-size distribution and, thus, change the probability of forming tie-chains that play a crucial role in the fibrillation process. The tie-chain concentration also depends on the molecular weight M_w. Craze formation and craze growth are then also influenced by the molecular weight. As M_w increases, the degree of crystallinity in the material decreases. Thus, the fraction of the material in amorphous interlayers, in which craze nucleation can take place, is increased. This leads to an increase in the number of crazes, an effect that is enhanced if the sample molecular weight is increased. The molecular weight has very little influence on the elastic-deformation behavior and on the stress or strain at which crazes are initiated. After craze initiation, stronger fibrils are formed, and they can grow with increasing stress and time. In general, the maximum fibril length increases with increasing molecular weight. This provides the observed increase in fracture strain. The forces transmitted by the fibrils grow with M_w due to a higher amount of topological entanglements between the crystalline blocks in the craze fibrils. This is reflected by the observed increase in breaking stress with increasing M_w. Under these conditions, the relevant stress is not the applied stress but the true fracture stress in the craze fibrils. Even though much energy is dissipated in the crazes, it is recognized that, when uncontrolled, crazes usually fracture and cause brittle behavior. However, when crazing is properly controlled, it can lead to substantial levels of toughness.

Polymers can behave in a brittle or in a ductile manner, depending on the testing conditions (temperature and strain rate) and their ability to resist craze formation and crack propagation. Linear elastic fracture mechanics (LEFM) has long been used to describe the failure of polymers under brittle fracture conditions.[2–4] The conditions under which the LEFM approach is applicable put severe constraints on the specimen dimensions. The size of the plastic zone must be smaller than the thickness of the specimen, a condition difficult to achieve in thermoplastics, especially in polyolefins. Fracture properties are usually expressed in terms of the *critical stress intensity factor,* K_c. In impact testing,[5] this quantity can be determined via the *strain energy-release rate,* G_c, that is calculated from the relationship

$$U = U_0 + G_c BD\Phi$$

where U is the fracture energy; U_0, a correction for kinetic energy loss; B, the thickness of the

sample; D, its width; and Φ, a geometric factor that may be taken from tables.[3] For IZOD and CHARPY impact tests, this factor depends on the ratio L/a, where L is the length of the sample and a is its thickness. The critical intensity factor K_c and the strain energy release rate, G_c, are related by

$$K_c^2 = E^* G_c$$

where $E^* = E$ (E is the elastic modulus) for plane stress conditions and $E^* = E/(1 - \nu^2)$ under plane strain conditions.

When full yielding occurs, the elastic analysis is no longer valid and the J-integral concept—a more general fracture energy criterion—may be used. Rice[6,7] developed an approach to the problem of identifying a unique parameter to characterize the failure of bodies with nonlinear and elastic behavior. Rice showed that a certain integral, now commonly called the J-integral, described the flow of energy into the crack-tip region. The J-integral is measured from the load-displacement curve. The characteristic value J_c is obtained by extrapolation of the linear part of the load-displacement curve. The quantity J_c is defined so that $J_c = G_c$ for the elastic case. Under conditions where more plastic behavior is occurring, it may be expressed in terms of the yield stress and the crack-tip displacement, u, using the equation

$$J_c = \sigma_y u$$

where σ_y is the yield stress. If full yielding is assumed in bending and this criterion is used,

$$U = \frac{u}{2} \sigma_y B(D - a) = J_c \frac{B(D - a)}{2}$$

where a is the notch depth. If the cross section of the notched sample is $A = B(D - a)$, then

$$J_c = \frac{2U}{A}$$

The factor of 2 arises because the average displacement in bending is $U/2$ compared with U in tension. The use of U/A as a parameter is, of course, a traditional way of analyzing fracture data, but the factor 2 must be introduced in bending to give valid comparisons with G_c.

Table I Number-average Molecular Weight, M_n, Weight-average Molecular Weight, M_w, and Polydispersity of Our Four Polymers

	M_n	M_w	Polydispersity
PP-homo	50,000	250,000	5
PP-copo	55,000	340,000	6.2
HDPE-homo	17,000	195,000	12
HDPE-copo	31,000	75,000	2.4

M_n and M_w were determined by gel-permeation chromatography (GPC) at Borealis.

SAMPLES

Our study was focused on polyethylene and polypropylene. Polyolefin plastics are all partially crystalline, with crystallinities varying from 40 to 50% to over 90%. The crystalline density is greater than is the amorphous density in these and most other materials. This leads to higher stiffness, tensile strength, heat resistance, yield resistance, hardness and lower permeability, stress crack resistance, impact resistance, and tear strength. Low-density polyethylene (LDPE) is usually used when flexibility and toughness are desired, whereas high-density polyethylene (HDPE) finds utility when hardness, rigidity, and higher strength are important.

Four different materials (see Table I), supplied by Borealis a/s (Ronningen, Norway), were chosen because of their relatively simple composition and their industrial interests: two polypropylenes referred to as PP-homo (a homopolymer) and PP-copo (a heterophasic propylene–ethylene copolymer) and two high-density polyethylenes referenced as HDPE-homo (a homopolymer) and HDPE-copo (a randomly distributed ethylene–hexene copolymer).

The specimens were prepared either by injection molding (PPs) or by hot pressing (PPs and PEs). The injection-molding cycle can be described as follows:

The polymer was injected into the mold at a controlled speed (injection time 2–3 s) and high temperature 200°C—well above the melt temperature). The mold temperature was 40°C and the holding pressure needed to avoid sink marks usually ranged from 200 to 500 bars and was applied for 40 s. The specimen was then cooled for 8 s (without applied pressure) and was ejected. The total cycle time was about 60 s. Because of the high viscosity in the molten phase, the PEs that

Table II Spherulites Size in the Center and Along the Edge of the Fracture Surface

	Central Part	Along the Edge	Crystallinity
PP-homo (inj.)	60 μm	17 μm	49.4%
PP-copo (inj.)	30 μm	20 μm	43.8%
PP-copo (h.p.)	55 μm	45 μm	46.2%
HDPE-homo (h.p.)	32 μm	25 μm	57.5%
HDPE-copo (h.p.)	—	—	72.4%

"inj." indicates that specimens were injection-molded, whereas "h.p." indicates that specimens were hot-pressed.

were studied could not be injection-molded, and, therefore, a hot press was used. Pellets were placed between two metallic plates, which were then placed in the press. The cycle started with a subcycle of compressions–decompressions during the melting of the pellets, to avoid air bubbles in the final sheets and to evaporate solvent traces. The polymer plate was then compressed for 10 min at 180°C (5 min at low pressure and 5 min at high pressure). A cool-down rate of 15°C/min was then applied until a temperature of 40°C was reached. The hot press was also used to prepared the PP samples, the only change being the compression temperature, which was 210°C.

All our specimens had the same shape: 10 × 80 mm with a thickness of 4 mm. To initiate fracture propagation in a specific location, the sheets were notched in one of the 4 × 80 mm faces (2 mm deep with a tip radius of 0.5 mm) when the experiments were performed.

The influence of the morphology on the fracture performance of PP and PE was described in the literature.[2,8–11] It appears that the fracture performance is strongly influenced by the processing conditions, which affect the supermolecular structure. Different crystalline morphologies (characterized by the tie-chain density, crystallinity, lamellar structure, and lamellar thickness) are associated with different thermal histories. All these parameters are interdependent, and it is not a simple matter to separate their respective effects. Nevertheless, some trends are apparent.

In our study, crystal sizes were measured with a cross-polarized light microscope. Thin slices (typically 10 μm) were microtomed. Pictures were taken at different locations on the slices, to explore the influence of cooling rates and mechanical deformation rates during processing. The results are summarized in Table II.

The injection-molding process induces a broader crystal-size distribution than does hot-pressing. This is not surprising since, as discussed previously, raw material is injected into the mold at a controlled speed and high temperature (≈200°C). The melting-point temperature of the two injection-molded polymers (PPs) are close to 160°C. The injection-molding process exposed the polymer to high-temperature gradients and high shear strain rates near the boundaries of the specimen and lower-temperature gradients and shear strain rates in the interior. This caused the crystallite sizes to be larger in the center of the specimen than along the edges. The relatively short duration of the injection-molding cycle did not allow time for extensive spherulite growth. During the hot-press process, samples were submitted to a much more gradual heat treatment, to keep the temperature as uniform as possible throughout the sample. This explains why, for a given material (PP-copo), the crystal sizes were larger and the size distribution was narrower in the hot-pressed specimens. Even though the spherulite size could not be measured precisely for the HDPE-copo sample (randomly distributed ethylene–hexene copolymer), it was found to be approximately 1 μm.

It is known that an increase in crystallinity usually induces a lowering of material toughness (the yield stress and the brittleness increase). When the crystallinity decreases, the crystal size decreases at the same time, which increases the probability of forming tie-chains (the average thickness of the crystals is reduced and, as a result, the average distance between crystals is reduced). Tie-chains join the crystals together to form a network. They play a crucial role in the molecular disentanglement process that takes place during fracture propagation (they increase the failure time) and their concentration appears to be a more important parameter than the crystal size itself.

The tie-molecule concentration also depends on the molecular weight M_w and on the short-chain branch density. Short-chain branches reduce the average thickness of crystals, increasing the tie-molecule concentration. They are also supposed to inhibit disentanglement processes, thus increasing the failure time. A detailed description of the supermolecular structure is needed to develop a more complete understanding, since the crystal size and size distribution provide only a partial characterization of these polymeric materials.

Table III Values of the Fracture Parameter J_c (kJ/m^2) at 23, 0, and −20°C Measured During the Charpy Test

	PP-homo (inj.)	PP-copo (inj.)	PP-copo (h.p.)	HDPE-homo (h.p.)	HDPE-copo (h.p.)
23°C	7.3 ± 0.6	20.5 ± 1.0	19.0 ± 1.0	18.6 ± 0.6 pb	41.5 ± 1.5 pb
0°C	2.5 ± 0.2	10.9 ± 0.3	11.1 ± 0.7	10.2 ± 0.3	46.0 ± 5.0 pb
−20°C	2.7 ± 0.7	8.5 ± 1.5	8.1 ± 0.8	9.0 ± 0.6	43.2 ± 1.5 pb

"inj." indicates that specimens were injection-molded, whereas "h.p." indicates that specimens were hot-pressed. "pb" indicates that the samples were partially broken.

RESULTS AND DISCUSSION

Temperature and Strain-rate Dependence

Fracture experiments were conducted at 23, 0, and −20°C to study the temperature dependence of the fracture surface structure and to generate fracture surfaces under different experimental conditions for identical samples. Some of the results are summarized in Tables III and IV. It can be seen that, for all samples but HDPE-copo, the fracture energy increases as the temperature is increased.

The fracture behavior of HDPE-copo seems to be temperature-independent. This is clearly shown in Figure 1. A very important parameter related to the mechanical properties of polymeric materials is the glass transition temperature, T_g. The glass transition temperatures were obtained from Borealis a/s. They are expected to be close to 0, −45, and 110°C, respectively, for the PP homopolymers, the PP/PE rubber phase, and HDPE. These values have to be taken with caution, because they have been measured at zero frequency ($\omega \rightarrow 0$) and T_g is known to be strain rate-dependent. It is very difficult to know precisely the strain rate in our fracture experiments, but an upper limit can be determined. In this type of impact tests, the fracture velocity is not controlled but measurements have shown that it increases in time until a maximum value (typically $\approx 0.5\ C_R$) is reached,[12–16] where C_R is the Rayleigh wave velocity (the velocity of a wave propagating on a free surface of a given material). It is possible to calculate C_R using the Rayleigh wave velocity equation[17]:

$$r^6 - 8r^4 + 8r^2(3 - 2s^2) - 16(1 - s^2) = 0$$

where $r = C_R/C_t$, $s = C_t/C_l$, and C_t and C_l are the transverse and longitudinal sound velocities. It was found that $C_R = 1210$ m/s for PP and $C_R = 900$ m/s for PE, at room temperature. This means that the approximate maximum value of the fracture propagation speed is 600 and 450 m/s for PP and PE, respectively. Taking into account the geometry of our samples, the maximum deformation rates in our experiments were estimated to be 7.5×10^4 s^{-1} for PP and 5.6×10^4 s^{-1} for PE. For polymers with a C—C backbone, it was determined that T_g increases by 5–8°C per frequency decade. The glass transition temperature is often determined using the storage and loss modulus–temperature curves obtained from rheological measurements. These measurements are performed at constant frequency, usually 1 Hz. Based on this observation, it is apparent that the effective value for T_g increases by up to 30–40°C in our fracture experiments, which is far from

Table IV Values of the Fracture Parameter J_c (kJ/m^2) at 23, 0, and −20°C Measured During Izod Test

	PP-homo (inj.)	PP-copo (inj.)	PP-copo (h.p.)	HDPE-homo (h.p.)	HDPE-copo (h.p.)
23°C	5.7 ± 0.3	19.0 ± 1.5	16.9 ± 0.8	24.0 ± 4.5 pb	38.0 ± 2.5 pb
0°C	3.20 ± 0.05	9.6 ± 0.5	11.4 ± 0.8	10.2 ± 0.9	40.5 ± 5.0 pb
−20°C	3.2 ± 0.5	8.5 ± 0.2	8.5 ± 1.0	9.0 ± 1.3	42.0 ± 5.0 pb

See footnote to Table III for abbreviations.

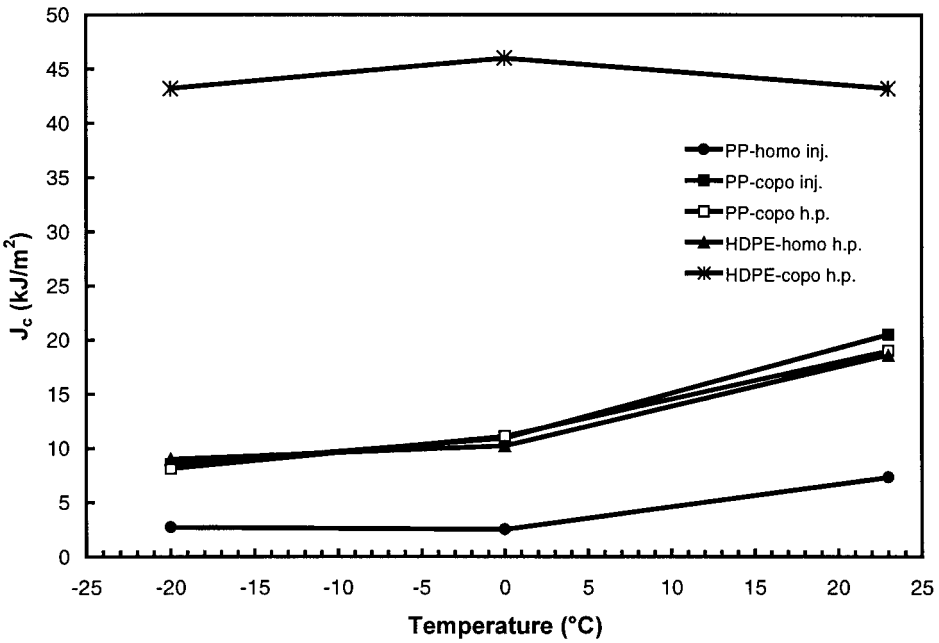

Figure 1 Evolution of J_c measured in Charpy experiments at different temperatures.

being negligible, indicating that for PP-homo, even for experiments conducted at 23°C, the material can behave as if it was below its T_g. Even if the fracture velocity does not reach 0.5 C_R, it is reasonable to believe that the effective T_g under our experimental conditions is much higher than the given (low-frequency) values.

If the temperature dependence (Fig. 1) of J_c determined for the PP-homo sample is examined, a transition in the fracture energy behavior is noticed at a temperature between 23 and 0°C. In this temperature range, J_c decreases by $\frac{2}{3}$ of its initial value, and it seems to remain constant at lower temperatures. This indicates that the T_g for the sample at the experimental strain rate is between 23 and 0°C. A slight discrepancy with the given value of T_g = 0°C, due to the high strain rate, is then noticed. A similar observation can be made for the PP-copo sample (PP/PE rubber phase) which has a low-frequency T_g value close to −45°C. A decrease in temperature from 23 to −20°C induced a 55% decrease in J_c. The shape of the J_c–temperature curve shows that J_c reaches a constant value and then becomes temperature-independent. This suggests that the T_g for PP-copo under our experimental conditions is close to −20°C. Once more, the discrepancy with the low-frequency value of −45°C is due to the high strain rate during fracture propagation. This effect should be taken into account in the choice of materials that will be subjected to a particular set of conditions (temperature, type of fracture, strain rate involved, etc.) during use.

Supermolecular Structure Dependence

We studied the influence of the supermolecular structure (more specifically, the crystal size, which was discussed in the third section—see Table II) on the mechanical properties. The energy to fracture versus crystal size is plotted in Figure 2. It can be clearly seen that the energy released during crack initiation and propagation is a decreasing function of the crystal size, in agreement with well-known trends. It was reported in the literature that spherulite size may not have a direct influence on the mechanical properties, but it is difficult to consider spherulite size independent of other effects. Some parameters that are expected to influence the mechanical behavior of polymers are summarized in Table V.

It can be seen that all these parameters are linked together. For a given polymer family (PP or PE), an increase in crystallinity induces an increase in density. Consequently, the crystal size becomes higher and the yield stress increases at the same time. All this leads to a lowering of J_c and the polymer becoming more brittle. Examination of the behavior of the polypropylene–ethylene copolymer (PP-copo) processed using two

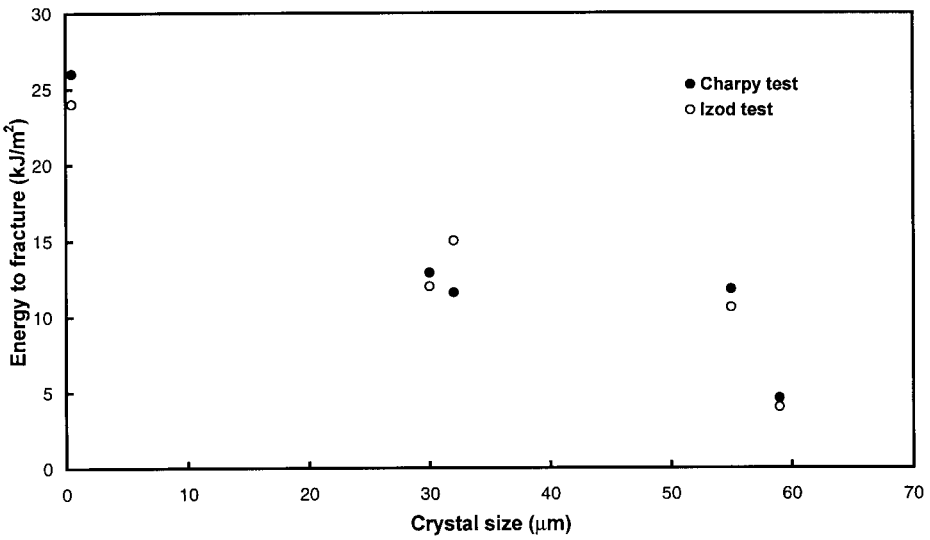

Figure 2 Plot of the energy released during crack initiation and propagation versus the crystals mean size obtained using data from Izod and Charpy tests.

different techniques [injection molding, PP-copo (inj.), and a hot press, PP-copo (h.p.)] indicates that they have different supermolecular structures. The injection-molded sample was submitted to a higher cooling rate, resulting in a lower crystallinity and smaller spherulites. This explains its higher impact resistance compared with the hot-pressed sample. However, it must be pointed out that, even if PP-copo (inj.) and PP-copo (h.p.) have two completely different histories, their impact resistances are quite similar. This suggests that heat treatment can be used to reach an optimal behavior but in a relatively narrow range of performance, whereas modification of the polymer chain structure (molecular weight, side chain length and density, introduction of blocks of different monomers) remains the most effective approach to achieving significant mechanical properties improvements. All these results should be confirmed by changing, gradually, the processing conditions, to obtain a wide range of supermolecular structures for each material.

Fracture-surface Microscopy and Qualitative Analysis

Our approach is to relate the structure of the fracture surfaces to the polymer structure and morphology, on the one hand, and to the mechanical properties, on the other. We tried to characterize qualitatively the rough surfaces generated by the fracture at three different temperatures (23, 0, and −20°C) for our five samples. A scanning electron microscope was used to visualize the fracture surfaces.

The fracture surface of the PP-homo PP appears to be quite regular with fine patterns, except along the edges and behind the notch. The

Table V Yield Stress σ_y, Density ρ, Crystallinity X, Crystallization Temperature, Melting Temperature, Crystal Size, and J_c (Charpy Test) for All Our Samples

Sample	σ_y (MPa)	ρ	X (%)	Crystallization/Melting Temperature (°C)	Crystal Size (μm)	J_c (kJ/m^2)
PP-homo	34.5	908	49.4	161.5/115.6	60/17	7.3
PP-copo (inj.)	25.5	902	43.8	163.0/115.6	30/20	20.5
PP-copo (h.p.)	—	—	46.2	161.9/120.0	55/45	19
HDPE-homo (h.p.)	29	957	72.4	134.4/120.2	32/25	18.6
HDPE-copo (h.p.)	16	936	57.4	123.7/111.3	—	41.5

The yield stress, density, and J_c were measured at room temperature.

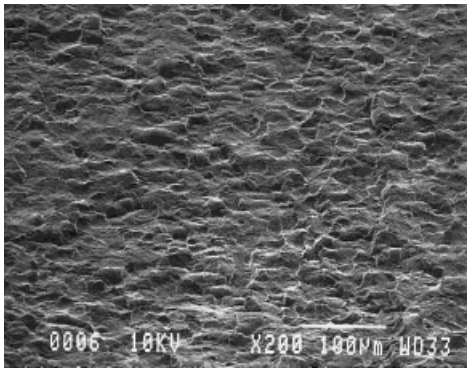

Figure 3 High-magnification SEM picture of a PP-homo sample. The experiment was performed at 23°C. The size of the image is 1 × 750 μm.

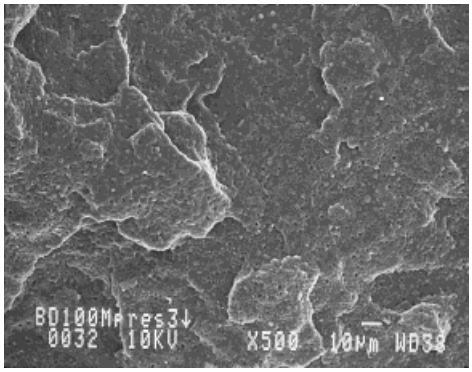

Figure 4 High-magnification SEM picture of a PP-copo sample. The experiment was performed at 23°C.

sheath along the edges consists of an outer-skin zone with a width of 100–150 μm and an inner shear zone with a width of 200–250 μm. The formation of these zones is a consequence of the injection-molding process used to form the specimen. The skin is formed as a result of rapid cooling during polymer processing, resulting in a small crystallite size and lower crystallinity. In the shear zone, oriented patterns can be observed. The differences between the shear zone and the bulk fracture morphologies are attributed to the effects of rapid shear deformation on the polymer morphology, near the surface of the sample during processing. PP is submitted to a shear stress to fill up the mold, leading to the observed orientation. In the central part of the fracture surface, fine regular patterns can be observed at both temperatures (see Fig. 3). No evidence of crazing or fibrillation can be observed, and the brittle fracture surface morphology does not seem to be temperature-dependent. Similar behavior, which can be interpreted in the same manner, was found for hot-pressed and injection-molded PP-copo copolymers. The fracture surfaces look qualitatively similar, with coarse patterns and surface morphologies characteristic of brittle failure (see Fig. 4), irrespective of the process and the temperature. The only temperature-dependent quantity may be the surface roughness which appears to be higher for hot-pressed specimens. To study the rms roughness, all the roughness measurements were performed over 0.5 × 1-mm regions (see Table VI). As for the homopolymer, no evidence of crazing or fibrillation was observed.

The fracture surfaces of HDPEs (HDPE-homo and HDPE-copo) were completely different. This reflects a much higher rate of plastic deformation, with crazing and fibrillation (see Figs. 5 and 6). Along the edges of the homopolymer, (HDPE-homo) fracture surface shear lips were detectable, with a maximum width of approximately 0.65 mm at room temperature. These are regions that underwent a pronounced ductile deformation as a result of the biaxial stress field present at the free surface of the specimen. The central part of the fracture surface remains the same at both temperatures, and its fine structure will be described later on. The only difference is the width of the shear lips, which seems to decrease with decreasing temperature. This may explain the decrease in fracture energy at low temperature.

Table VI Rms Roughness of Fracture Surfaces Generated at 23 and −20°C

	PP-homo (inj.)	PP-copo (h.p.)	HDPE-homo (h.p.)	HDPE-copo (h.p.)
Rms roughness (113m) 23°C	10.1	18.7	3.6	8.2
Rms roughness (113m) −20°C	8.0	8.9	3.1	7.5

The roughness was measured from 1 × 0.5-mm images.

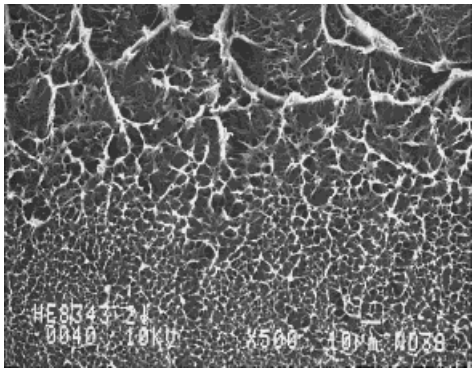

Figure 5 High-magnification SEM picture of a HDPE-homo sample. The experiment was performed at 23°C.

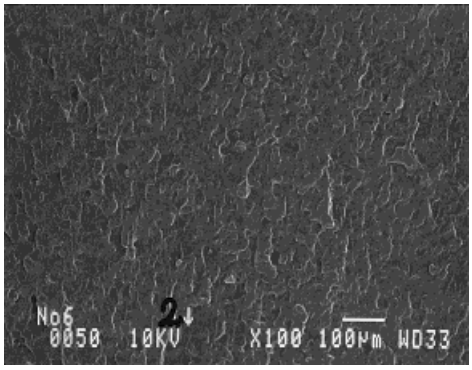

Figure 7 High-magnification SEM picture of a PP-homo sample. The experiment was performed at −20°C.

The block copolymer HDPE-copo was the sample with the highest fracture energy. For this sample, wide shear lips (with a maximum width close to 1 mm) could be observed surrounding the central part of the fracture surface, which is composed of crazed matter. The background of this region appeared to be relatively flat, with patterns resulting from crazing and fibrillation processes emerging from it. Just behind the notch, a semicircular region that differs from the bulk region could be seen. It represents the plastic zone at fracture initiation. Its size seems to be temperature-independent, with a radius close to 3 mm. The fracture surfaces looked the same at both temperatures.

Figures 3–11 show high-magnification SEM pictures of the central part of fracture surfaces formed at 23 and −20°C. For the PP homopolymer (PP-homo), brittle behavior was found at both temperatures, but the fracture surfaces appeared to differ slightly (see Figs. 3 and 7). At 23°C, the surface was relatively regular, with a rounded hill and valley relief. The relief is smooth in the sense that most of the peaks have a round shape and sharp edges are rare. Visual inspection shows that there is no evidence that fracture propagation occurs preferentially in the amorphous phase between spherulites. In Figure 8, the top of a spherulite emerging from the fracture surface can be clearly seen. However, this is not the common way for the fracture to propagate. This intact spherulite is surrounded by broken spherulites, showing that even if the amorphous matter is the weakest point of the structure the fracture does not follow the interfacial region between spherulites and the surrounding amorphous polymer, but tends to propagate in a more direct path, through the crystalline structure. At −20°C, the fracture also has a brittle character, but the fracture surface looks more damaged.

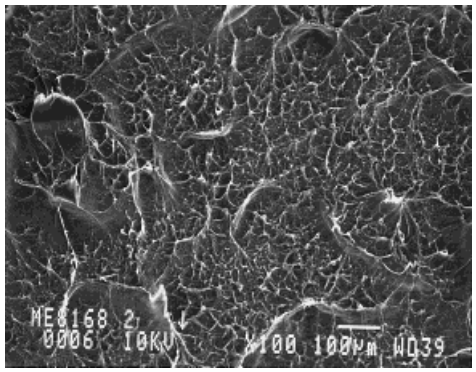

Figure 6 High-magnification SEM picture of a HDPE-copo sample. The experiment was performed at 23°C.

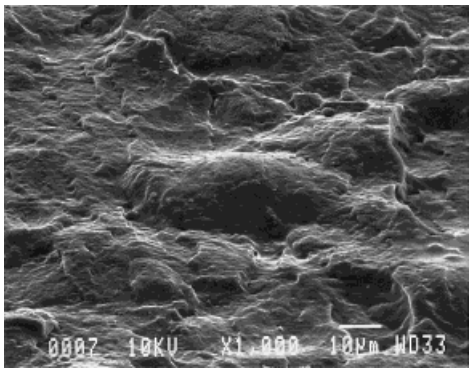

Figure 8 High-magnification SEM picture of a PP-homo sample. The experiment was performed at 23°C. The size of the image is 290 × 225 μm.

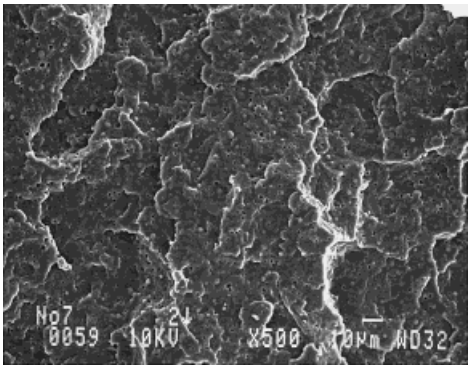

Figure 9 High-magnification SEM picture of a PP-copo sample. The experiment was performed at −20°C.

At room temperature, the fracture was described as "brittle" because of the lack of fibrils on the fracture surface. At −20°C, the fracture surface has lost its rounded hill and valley relief, and the patterns edges seem to be sharper than those obtained at higher temperatures. As mentioned previously, this change is directly linked to the glass transition, which occurred between room temperature and 0°C.

As for the homopolymer, Figures 4 and 9 indicate that the two-phase PP copolymer fractures in a brittle manner. The fracture surfaces look the same at both temperatures, and the process used to prepare the specimen does not seem to have any influence. Small black holes and white bumps can be observed on the PP-copo fracture surface, due to the heterophasic nature of the copolymer. The PP-copo materials consists of a blend of PE chains in a matrix of PP, in which the two phases are not linked together. The boundary between PE nodules and the PP phase is a weak point in the copolymer structure. When a crack propagates, these nodules are pulled out from the matrix, leaving holes on one of the fracture surfaces. Close inspection of the fracture surface indicated that the typical distance between nodules was in the 5–10 μm range.

PEs behave in a totally different way. They are much more ductile materials that undergo crazing and fibrillation processes. Evidence for crazing can be seen on the HDPE-homo fracture surfaces (Figs. 5 and 10), especially at room temperature. During crack propagation, small craters, with very well defined borders, were created on the fracture surface. The borders were made of crazed matter that was stretched in a direction perpendicular to the fracture plane. The surface was a result of the cavitation process occurring in the crazing zone and the breakdown of the stretched fibrils. The mean size of the craters should be related to the mean distance between two consecutive fibrils. It can be seen in Figure 5 that the crater pattern exists on a wide range of scales and could be observed at any magnification. The transition from a coarse structure to a fine structure is caused by irregular crack propagation, but it is remarkable that the coarse and fine structures look exactly the same. From a statistical point of view, they were identical. As the temperature was lowered from 23 to 0°C and then to −20°C, the fibrillation process gradually disappeared. This can be seen at high magnification, whereas the macroscopic aspect remains the same. At −20°C, the network of crazing-induced craters has disappeared. Traces of remaining fibrillation process can be observed on the edges of macroscopic patterns (the whitened parts in Fig. 10). One explanation may be that the high-frequency T_g of the polymer was close to the experimental temperature.

The fracture surface morphology of the HDPE copolymer (HDPE-copo) seems to be temperature-independent (see Figs. 6 and 11). As for the homopolymer, the fibrillation process created cavities. The main difference is that relatively large sheets of highly deformed matter were found in this fibrillation-induced network. Compared with the HDPE-homo specimen, the fibrils were thinner on the copolymer fracture surface. Careful inspection of pictures at the highest magnification showed that the typical size of the cavities or craters was in the 5–10-μm range. This also differs from the homopolymer behavior, for which it was impossible to identify characteristic features of any typical size.

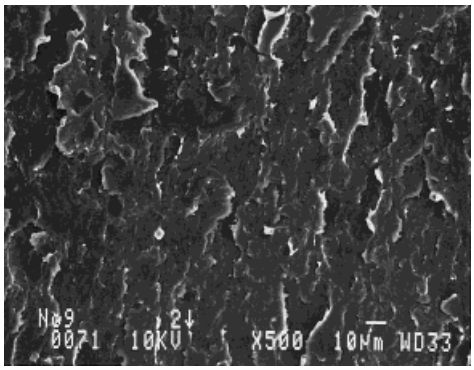

Figure 10 High-magnification SEM picture of a HDPE-homo sample. The experiment was performed at −20°C.

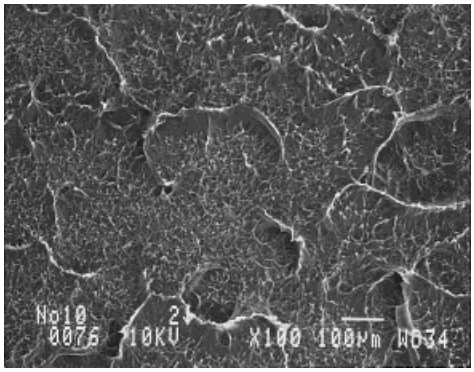

Figure 11 High-magnification SEM picture of a HDPE-copo sample. The experiment was performed at −20°C.

To obtain a more complete description of the fracture surfaces, thin slices (typically 10 μm thick) were cut perpendicular to the surface and parallel to the crack propagation direction. Samples were cut with a microtome and the razor blade was changed after every cut. By using a cross-polarized light microscope, the supermolecular structure beneath the fracture surface could be examined. It could then be determined if the initial structure was damaged after the crack propagation. Figures 12–15 confirm the brittle fracture of both PPs (PP-homo and PP-copo) and the characteristic morphology of the PE fracture surfaces (HDPE-homo and HDPE-copo). For the PP-homo specimen, it was clear that the fracture propagates through the spherulites, as Figure 12 indicates. The spherulites are broken in a very brittle manner; the remaining parts of the spherulites are apparently not deformed. The organization of the spherulites beneath the fracture surface does not seem to have been perturbed. A closer inspection showed that the fractures tended to pass through the spherulites, following a radial direction. This indicates that they passed through the centers of the spherulites (the nucleation point) and that the crack propagation was influenced by the orientation of the lamellae. At both 23 and −20°C, short cracks and partially broken spherulites can be seen. This brittle be-

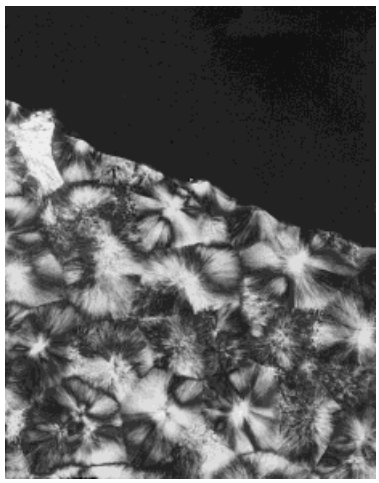

Figure 12 The supermolecular structure beneath the fracture surface of a PP-homo sample. The experiment was performed at 23°C. The cut is oriented perpendicular to the fracture surface and parallel to the fracture propagation direction. The size of the image is 290 × 225 μm.

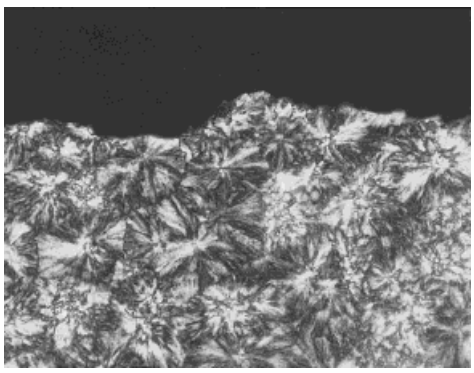

Figure 13 The supermolecular structure beneath the fracture surface of a PP-copo sample. The experiment was performed at 23°C. The cut is oriented perpendicular to the fracture surface and parallel to the fracture propagation direction. The size of the image is 290 × 225 μm.

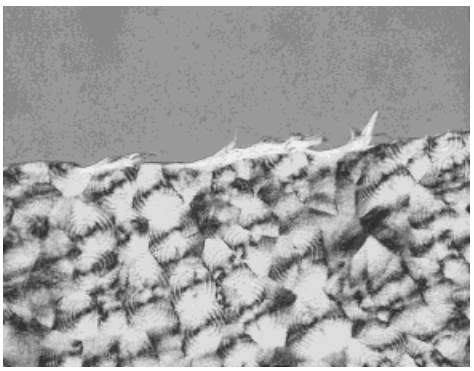

Figure 14 The supermolecular structure beneath the fracture surface of an HDPE-homo sample. The experiment was performed at 23°C. The cut is oriented perpendicular to the fracture surface and parallel to the fracture propagation direction. The size of the image is 290 × 225 μm.

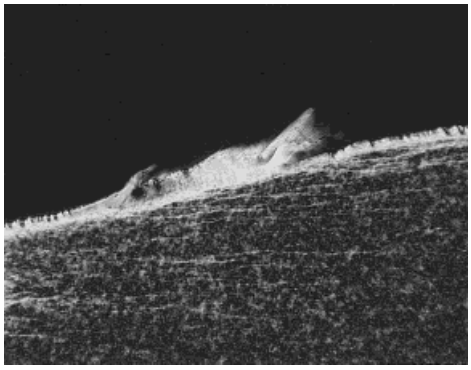

Figure 15 The supermolecular structure beneath the fracture surface of an HDPE-copo sample. The experiment was performed at 23°C. The cut is oriented perpendicular to the fracture surface and parallel to the fracture propagation direction. The size of the image is 290 × 225 μm.

havior is not surprising. At room temperature, many semicrystalline thermoplastics are above their glass transition points, and they owe their strength and stiffness to crystalline phases. During the early stages of deformation, the deformation process takes place mainly in the the relatively soft amorphous layers. But the stress–strain curve is largely determined by the presence and arrangement of the crystals. Interlamellar slip has been identified as an important deformation mechanism. On the other hand, when the temperature is lowered (or when experiments are conducted at very high strain rates), deformation within the amorphous phase becomes more and more restrained, and the material is expected to behave more like a glassy polymer. This is exactly what we found for the two PPs.

The transverse cut of the PP-copo fracture surface (see Fig. 13) confirms the brittle behavior of the material. The fracture goes through spherulites, and the fracture surfaces generated at 23 and −20°C appear to be very similar.

Figure 15 confirms the totally different behavior of the copolymer HDPE-copo. The presence of a white band along the fracture surface, with an approximately constant thickness, is a consequence of the drawing process that occurs during crazing. Usually, crazes grow by drawing material from the matrix. This leads to a change in micromorphology in a layer called the active zone. When a fibril breaks, it forms a dimple in the fracture pattern. The thickness of the active zone is approximately 10–12 μm at 23°C and 5–7 μm at −20°C. At 23°C, parallel white lines can be seen in the bulk, under the fracture surface, and they are called strain lines. Their white color indicates that the microstructure along these lines has changed due to the concentration of stress along a well-defined line. They may consist of crazes that have not developed into cracks or shear bands. In both cases, their presence shows that the crack propagation induces a more global (less localized) deformation in the specimen than for the PP specimens. This is due to a lower glass transition temperature, which leads to a softer material behavior. These bands are not visible at −20°C, but this may be because of a different light polarization that could have masked the oriented patterns.

Like the PP fractures, the fracture propagates through the spherulites in the HDPE homopolymer (Fig. 14). However, for the HDPE homopolymer, fibrils emerging from the broken spherulites can also be seen. At 23°C, the active zone was limited in size and did not spread all over the fracture surface. In Figure 14, material that was dragged from the spherulites to form the active zone can be clearly seen. It is surprising that the crystalline-ordered structure was not destroyed during this process. At −20°C, the local active zones disappeared, and some fibrils remained on the fracture surface. No strain bands were observed, since the glass transition temperature of the specimen was too close to the temperatures of the experiments.

CONCLUSIONS

The goal of this work was to study the structure of fracture surfaces in order to discover correlations between quantitative measures of the polymer structure and the mechanical properties of the final products. The fracture was shown to propagate through the spherulites and followed the lamellae orientation in the PP homopolymers. In terms of fracture toughness, heat treatment can be used to improve mechanical properties but these variations are small. The best way to achieve superior properties is to modify the chemical structure.

The temperature and strain rate are very important parameters in the control of crack propagation. The energy to fracture increases with temperature, as does the fracture surface roughness (but only slightly). The rms roughness measured over 1 × 0.5-mm areas was approximately 20% higher for fracture surfaces generated 23°C com-

pared with those generated at −20°C. The strain rates involved in fracture processes greatly influence the material behavior, by changing its effective glass transition temperature to behave as glassy polymers at temperature 20–30°C higher than the low frequency T_g. This has to be taken into account in the choice of polymers, depending on the conditions that the final products will be exposed to and the manner in which the material will fail (low strain rate subcritical fracture propagation or high strain rate supercritical fracture propagation).

Our measurements have shown that a decrease in temperature leads to a decrease of 20% in the rms roughness when it is measured over 1 × 0.5-mm areas and a lower fracture energy (except for the HDPE-copo sample). At the same time, fracture surfaces at 23°C are very similar to those generated at −20°C, even though the fracture energy changes a lot. The small variations in the rms roughness and the fracture surface topography do not explain the observed changes in toughness. The fracture surfaces are very complex and are composed of a central region and side regions (e.g., skin and shear bands). The size of each region seems to be temperature-dependent, and this could explain the change in fracture energy with the temperature. It should be rewarding to studying the structure of each part individually (not only in the central part which was the focus of our work) and try to correlate it with the energy dissipated. The change in fracture energy, while the geometry of the fracture surfaces remains almost the same, could also indicate that only a small amount of the energy is used to create the new free surfaces, the rest being dissipated by deformation processes occurring in the bulk of the specimens. Further investigations are needed to obtain a better understanding of this issue.

This work was supported by the Norwegian Research Council. The authors would like to thank Borealis AS for providing the samples and for use of their mechanical testing equipment. We would like to acknowledge Karstein Kleveland (Borealis AS) for encouraging and coordinating the collaboration with Borealis AS.

REFERENCES

1. Kausch, H. H. Advances in Polymer Science; Springer-Verlag: New York, 1983; Vols. 52/53.
2. Ouerdini, M.; Phillips, P. J. J Polym Sci Part B Polym Phys 1995, 33, 1313–1322.
3. Williams, J. C. Fracture Mechanics of Polymers; Ellis Horwood: Chichester, 1984.
4. Pukanzky, B.; Maurer, F. H. J.; Boode, J. W. Polym Eng Sci 1995, 35, 1962–1971.
5. Plati, E.; Williams, J. C. Polym Eng Sci 1975, 15, 470–477.
6. Rice, J. R. J Appl Mech 1968, 35, 379.
7. Leibowitz, H. In Fracture, An Advanced Treatise; Academic: New York, 1979.
8. Frontini, P. M.; Fave, A. J Mater Sci 1995, 30, 2446–2454.
9. Sugimoto, M.; Ishikawa, M. Polymer 1995, 36, 3675–3682.
10. Lu, X.; Qian, R.; Brown, N. Polymer 1995, 36, 4239–4244.
11. Zhou, Z.; Brown, N. Polymer 1994, 35, 3619–3623.
12. Gross, S. P. Ph.D. Thesis, University of Texas, Austin, 1995.
13. Sharon, E.; Gross, S. P.; Fineberg, J. Phys Rev Lett 1995, 74, 5096–5099.
14. Sharon, E.; Gross, S. P.; Fineberg, J. Phys Rev Lett 1996, 76, 2117–2120.
15. Fineberg, J.; Gross, S. P.; Marder, M.; Swinney, H. L. Phys Rev Lett 1991, 67, 457–460.
16. Fineberg, J.; Gross, S. P.; Marder, M.; Swinney, H. L. Phys Rev B 1992, 45, 5146–5154.
17. Pollard, H. F. Sound Waves in Solids; Pion: London, 1977.